

Hybrid iLQR Model Predictive Control for Contact Implicit Stabilization on Legged Robots

Nathan J. Kong¹, Chuanzheng Li², and Aaron M. Johnson¹

Abstract—Model Predictive Control (MPC) is a popular strategy for controlling robots but is difficult for systems with contact due to the complex nature of hybrid dynamics. To implement MPC for systems with contact, dynamic models are often simplified or contact sequences fixed in time in order to plan trajectories efficiently. In this work, we extend Hybrid iterative Linear Quadratic Regulator to work in a MPC fashion (HiLQR MPC) by 1) modifying how the cost function is computed when contact modes do not align, 2) utilizing parallelizations when simulating rigid body dynamics, and 3) using efficient analytical derivative computations of the rigid body dynamics. The result is a system that can modify the contact sequence of the reference behavior and plan whole body motions cohesively – which is crucial when dealing with large perturbations. HiLQR MPC is tested on two systems: first, the hybrid cost modification is validated on a simple actuated bouncing ball hybrid system. Then HiLQR MPC is compared against methods that utilize centroidal dynamic assumptions on a quadruped robot (Unitree A1). HiLQR MPC outperforms the centroidal methods in both simulation and hardware tests.

Index Terms—Legged Robots, Model Predictive Control, Hybrid Dynamics, Whole Body Motion Planning

I. INTRODUCTION

In order for robots to reliably move and interact within our unstructured world, they need to be able to replan motions to handle unexpected perturbations or changes in the environment. However, replanning is difficult for robotic systems that have changing contact with the world because of the complexity of the discontinuous dynamics and combinatoric issues that arise.

There are many methods for planning contact-rich behaviors offline [1–4], but these methods generally suffer from poor time complexity and cannot be used directly in real-time applications. Direct methods for contact implicit trajectory optimization [1,2] simultaneously solve for the states, inputs, and contact forces of an optimal trajectory while encoding the contact conditions through complementarity constraints – which are notoriously difficult and slow to solve. A relaxation of contact implicit trajectory optimization is to fix the contact sequence for each timestep [5–9].

Other relaxations have been made for the planning problem to achieve real-time planning for Model Predictive Control (MPC). Centroidal motion planning methods [10–14] have had a lot of success in planning gaits in real-time by making large simplifications on the robot dynamics and also assuming a

fixed contact sequence a priori. Swing legs are often controlled separately using Raibert heuristics [15] and capture point methods [16] to regulate body velocities. However, simplifications to the robot dynamics can lead to the controller being less robust to perturbations which require reasoning about the full dynamics, such as nonlinear changes in lever arm for leg extension, varying inertia when the leg changes shape, or not accounting for unexpected changes in contact.

Shooting methods which utilize Differential Dynamic Programming (DDP) [17] or iterative Linear Quadratic Regulator (iLQR) [18,19] are good candidates for model predictive control because they are fast, can utilize the full nonlinear dynamics, and solutions are always dynamically feasible. Methods that utilize the full nonlinear dynamics [20,21] generally come at the cost of enforcing a fixed contact sequence. [22] utilizes the full nonlinear dynamics for timesteps closer to the current horizon and then uses simplified dynamics for timesteps later in the future, but also uses a fixed contact sequence. Similar to the fixed contact sequence issue of [10], it is less robust due to constraining the solution to maintain the original contact sequence in scenarios where it would be much better to change them.

To allow efficient updates of the contact sequence, [23] speeds up contact implicit trajectory optimization through strategic linearizations about a target trajectory and focuses on the tracking problem, which allows the possibility of running in real time and can easily change the contact timing and sequence to stabilize a trajectory. However, the basin of attraction may be smaller because it is linearized about a single nominal trajectory. If the robot needs to drastically change the trajectory, the controller will not use a good model given the linearization of the target trajectory.

In this work, we make use of Hybrid iLQR (HiLQR) [24], a full-order contact implicit trajectory optimization approach, in order to create a receding horizon MPC that utilizes nonlinear dynamics and is not constrained to the reference trajectory’s gait sequence. By using Hybrid iLQR as an MPC, the contact sequence can be greatly modified when stabilizing large perturbations, e.g. as shown in Fig. 1. We show that HiLQR MPC can reject bigger disturbances than centroidal methods when perturbed along a walking trajectory. We also show that HiLQR MPC working on a real robot in real-time can reject disturbances more reliably than centroidal methods.

II. HYBRID SYSTEMS BACKGROUND

In this section, we define what a hybrid system is and the first order linearization for hybrid events. Also, two different

Corresponding author N. J. Kong njkong@andrew.cmu.edu.

¹ Department of Mechanical Engineering, Carnegie Mellon University, Pittsburgh, Pennsylvania

² XPeng Robotics, Mountain View, California

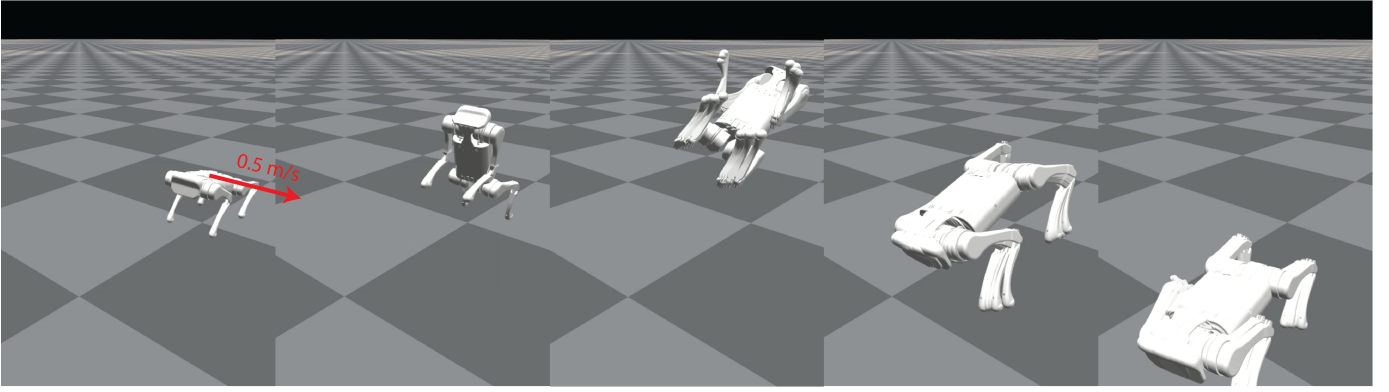


Figure 1: HiLQR MPC forward pass for tracking a backflip with an initial 0.5 m/s lateral perturbation on the body. 9 robot models are used on the forward pass to solve the line search in parallel.

hybrid simulation techniques are reviewed for rigid body systems with unilateral constraints.

A. Hybrid Systems

This section closely follows the formulation of hybrid systems from [24,25].

Definition 1: A **hybrid dynamical system** [26–28] is a tuple $\mathcal{H} := (\mathcal{J}, \Gamma, \mathcal{D}, \mathcal{F}, \mathcal{G}, \mathcal{R})$ where the parts are defined as:

- 1) $\mathcal{J} := \{I, J, \dots, K\} \subset \mathbb{N}$ is the finite set of discrete **modes**.
- 2) $\Gamma \subset \mathcal{J} \times \mathcal{J}$ is the set of discrete **transitions** that form a directed graph structure on \mathcal{J} .
- 3) \mathcal{D} is the collection of **domains** D_I .
- 4) \mathcal{F} is a collection of time-varying **vector fields** F_I .
- 5) \mathcal{G} is the collection of **guards** where $G_{(I,J)}(t) = \{(x, t) \in D_I | g_{(I,J)}(t, x) \leq 0\}$.
- 6) \mathcal{R} is called the **reset** that maps the state from D_I to D_J when the guard $G_{(I,J)}$ is met.

An example hybrid execution may consist of a starting point x_0 in D_I flowing with dynamics F_I and reaching the guard condition $g_{(I,J)}(x, t) = 0$, applying the reset map $R_{(I,J)}(x, t)$ resetting into D_J and then flowing with the new dynamics F_J .

Definition 2: The **saltation matrix** [29–32]

$$\Xi := D_x R + \frac{(F_J - D_x R \cdot F_I - D_t R) D_x g}{D_t g + D_x g \cdot F_I} \quad (1)$$

is the first order approximation of the variational update at hybrid transitions from mode I to J evaluated at time t , pre-impact state $x(t^-)$, and control input $u(t^-)$, with F_I evaluated at $F_I(t^+, x(t^-), u(t^-))$ and F_J evaluated at $F_J(t^+, x(t^+), u(t^-))$, and where $x(t^+) = R_{(I,J)}(t^-, x(t^-))$. It maps perturbations to first order from pre-transition $\delta x(t^-)$ to post-transition $\delta x(t^+)$ in the following way

$$\delta x(t^+) = \Xi \delta x(t^-) + \text{h.o.t.} \quad (2)$$

where *h.o.t.* represents higher order terms.

B. Hybrid Simulators

There are 2 main hybrid simulation techniques for rigid bodies with unilateral constraints – event-driven and timestepping. HiLQR MPC uses a hybrid simulator and can use

either method. But different modifications need to be made depending on which simulation type is used. Its important to have a high level understanding of each of these simulation types to understand that modifications discussed in this work.

Event-driven hybrid simulators [33–35] follow very closely to the example shown in the definition of hybrid dynamical systems Def. 1. Event-driven simulations are convenient because the dynamics have a well defined structure and contacts are persistently maintained. However, event-driven simulations have problems with behaviors like Zeno, where an infinite number of hybrid transitions are made in a finite amount of time, as they must stop integration and apply a reset map for each individual event.

Time-stepping [35–37] schemes circumvent issues like Zeno by integrating impulses over small timesteps at a time and are numerically efficient, especially for systems with large numbers of constraints. These methods allow contact constraints to be added or removed at any time step, but only once per time step. Furthermore, no distinction is made between continuous contact forces and discontinuous impulses. However, they are limited to first-order (Euler) integration of the dynamics.

III. HYBRID iLQR

This section reviews important equations from Hybrid iLQR [24]. The overall Hybrid iLQR algorithm consists of simulating hybrid dynamics for the forward pass and then using the variational equations of the hybrid dynamics on the backward pass to find stabilizing gains and direction of improvement. For a more detailed derivation, see [24].

Consider a hybrid trajectory with states $x \in \mathbb{R}^n$, inputs $u \in \mathbb{R}^m$, dynamics $\dot{x} = F(x(t), u(t))$, reset maps $x^+ = R(x^-)$, and guard surfaces $g(x^-) = 0$. Note that we assume that the correct dynamics, guards, and reset maps are selected for each timestep. Define a discretization of the continuous dynamics over a timestep Δ such that at time t_k the discrete dynamics are $x_{k+1} = f_\Delta(x_k, u_k)$, where $t_{k+1} = t_k + \Delta$, $x_k = x(t_k)$, and $u_k = u(t_k)$. If a hybrid event is triggered anytime during a discrete update, the appropriate hybrid update is applied. Without loss of generality, assume at most one hybrid change occurs during a single timestep. In this case, the sub-timestep before the hybrid transition is Δ_1 and the sub-timestep after

the hybrid transition is Δ_2 . Let $U := \{u_0, u_1, \dots, u_{N-1}\}$ be the input sequence, J_N the terminal cost, and J the runtime cost, where J and J_N are differentiable functions. The optimal control problem over a time horizon of N timesteps is

$$\min_U J_N(x_N) + \sum_{i=0}^{N-1} J(x_i, u_i) \quad (3)$$

$$\text{where } x_0 = x(0) \quad (4)$$

$$x_{i+1} = f_\Delta(x_i, u_i) \quad \forall i : g(x_i, u_i) > 0 \quad (5)$$

$$x_{i+1} = f_{\Delta_2}(R(f_{\Delta_1}(x_i, u_i))) \quad \forall i : g(x_i, u_i) = 0 \quad (6)$$

where $g(x_i, u_i) = 0$ signifies whether a hybrid event occurred during timestep i .

To solve this problem, Hybrid iLQR uses Bellman recursion to find the optimal input sequence U where $U_k := \{u_k, u_{k+1}, \dots, u_{N-1}\}$ is defined as the sequence of inputs including and after timestep k . The cost-to-go J_k is defined to be the cost incurred including and after timestep k

$$J_k(x_k, U_k) := J_N(x_N) + \sum_{i=k}^{N-1} J(x_i, u_i) \quad (7)$$

The value function V (Bellman equation) at state x_k is the optimal cost to go $J_k(x_k, U_k)$, which can be rewritten as a recursive function of variables from the current timestep using the dynamics (5)–(6)

$$V(x_k) := \min_{u_k} J(x_k, u_k) + V(f_\Delta(x_k, u_k)) \quad (8)$$

The boundary condition of the value is the terminal cost $V_N(x_N) := J_N(x_N)$. For clarity, define Q_k to be the argument optimized in (8). The resulting function is defined to be

$$Q_k(\delta x, \delta u) := J(x_k + \delta x, u_k + \delta u) - J(x_k, u_k) + V(f_\Delta(x_k + \delta x, u_k + \delta u)) - V(f_\Delta(x_k, u_k)) \quad (9)$$

where the value function expansion is for timestep $k + 1$. Hybrid iLQR uses a second order local approximation of Q_k where variations about the current state and input pair (x_k, u_k) are taken and when expanded to second order Q_k is approximated to be

$$Q_k(\delta x, \delta u) \approx \frac{1}{2} \begin{bmatrix} 1 \\ \delta x \\ \delta u \end{bmatrix}^T \begin{bmatrix} 0 & Q_x^T & Q_u^T \\ Q_x & Q_{xx} & Q_{ux}^T \\ Q_u & Q_{ux} & Q_{uu} \end{bmatrix} \begin{bmatrix} 1 \\ \delta x \\ \delta u \end{bmatrix} \quad (10)$$

The terms for each expansion coefficient are shown

$$Q_{x,k} = J_x + f_{x,\Delta}^T J_{x,N_j} + f_{x,\Delta}^T \Xi^T V_x \quad (11)$$

$$Q_{u,k} = J_u + f_{u,\Delta}^T J_{x,N_j} + f_{u,\Delta}^T \Xi^T V_x \quad (12)$$

$$Q_{xx,k} = J_{xx} + f_{x,\Delta}^T J_{xx,N_j} f_{x,\Delta} + f_{x,\Delta}^T \Xi^T V_{xx} \Xi f_{x,\Delta} \quad (13)$$

$$Q_{ux,k} = J_{ux} + f_{u,\Delta}^T J_{xx,N_j} f_{x,\Delta} + f_{u,\Delta}^T \Xi^T V_{xx} \Xi f_{x,\Delta} \quad (14)$$

$$Q_{uu,k} = J_{uu} + f_{u,\Delta}^T J_{xx,N_j} f_{u,\Delta} + f_{u,\Delta}^T \Xi^T V_{xx} \Xi f_{u,\Delta} \quad (15)$$

where $J_* = D_* J$ and $f_{*,\Delta} = D_* f_\Delta(x, u)$ for $* \in \{x, u\}$. Note that a simplification we make for the expansion is that we assume that the hybrid transition occurs at the end of the timestep to ensure piecewise smooth control inputs. In the absence of a hybrid transition, the coefficient expansion is the smooth iLQR update, and the saltation matrices Ξ are

removed. The remaining steps of the backward pass are exactly the same as standard iLQR, because the hybrid terms are now encoded in the coefficient expansion.

The optimal control input, δu^* , can now be found by setting the derivative of $Q(\delta x, \delta u)$ with respect to δu to zero and solving for δu

$$\delta u^* = \arg \min_{\delta u} Q(\delta x, \delta u) = -Q_{uu}^{-1}(Q_u + Q_{ux}\delta x) \quad (16)$$

This term can be split into a feedforward term $u_{ff} = -Q_{uu}^{-1}Q_u$ and a feedback term $K = -Q_{uu}^{-1}Q_{ux}\delta x$. Therefore, the optimal input for the local approximation at timestep k is the sum of the original input and the optimal control input, $u_k^* = u_k + \delta u^*$. The Bellman update for the expansion of V for timestep k is updated by inserting the optimal controller into (10)

$$V_x = Q_x - Q_u Q_{uu}^{-1} Q_{ux} \quad (17)$$

$$V_{xx} = Q_{xx} - Q_{ux}^T Q_{uu}^{-1} Q_{ux} \quad (18)$$

Now that the expansion terms for the value function at timestep k can be expressed as the sole function of $k + 1$, the optimal control input can be calculated recursively and stored $(u_{ff,k}, K_k)$. This process is called the backward pass. The convergence of the algorithm is determined by when the magnitude of the total expected reduction δJ is small

$$\delta J(\alpha) = \sum_{i=0}^{N-1} u_{ff,i}^T Q_{u,i} + \frac{1}{2} \sum_{k=0}^{N-1} u_{ff,i}^T Q_{uu,i} u_{ff,i} \quad (19)$$

The forward pass can modify the hybrid mode sequence, and there can be an issue with tracking a previous iteration's trajectory where it does not match the hybrid mode of the current state. This mode mismatch can lead to very large errors in state and result in bad solutions. A fix for this is to use reference extensions where the reference is extended past the guard by integration, and the gains and inputs are held constant for those times. Now, if there is a mode mismatch, one of the extensions can be used instead of the original reference to ensure that there is no mode mismatch.

An iteration of Hybrid iLQR consists of initializing the algorithm with a hybrid rollout to create an initial hybrid trajectory, then a backward pass is used to schedule feedforward and feedback gains, then several hybrid forward passes are implemented in a linesearch fashion with a learning parameter on the feedforward gain. The backward pass and forward pass linesearch are repeated until convergence.

IV. HiLQR MPC IMPLEMENTATION

In this section, the tracking problem is defined, and we show how to adapt Hybrid iLQR to be a model predictive controller.

A. Hybrid Cost Update

The goal is now to minimize the difference in state and input with respect to a reference state and input

$$J(x_i, u_i) = (x_i - \hat{x}_i)^T Q_i (x_i - \hat{x}_i) + (u_i - \hat{u}_i)^T R_i (u_i - \hat{u}_i) \quad (20)$$

where Q_i is the quadratic penalty matrix on state, and R_i is the quadratic penalty matrix on input, and (\hat{x}, \hat{u}) denotes the reference.

However, because Hybrid iLQR is contact implicit (the hybrid mode sequence can differ from the target’s mode sequence), the runtime cost (20) can be ill defined when the candidate trajectory’s mode does not match the target’s. For example, if there is an early or late contact in a rigid body system with unilateral constraints, the velocities will be heavily penalized for having a mismatched timing. This issue is further propagated to the backward pass, where the gradient information relies on these differences and can ultimately lead to the algorithm not converging. To mitigate these mode mismatch issues, we propose 2 different solutions for event-driven and timestepping simulations.

For event-driven hybrid simulators, the same hybrid extensions used in reference tracking on the forward pass in Hybrid iLQR can be used when comparing error during mode mismatches. Suppose a hybrid transition occurs at time t . The reference state at pre-transition $\hat{x}(t^-)$ is extended beyond the hybrid guard by flowing the pre-transition dynamics forwards while holding the pre-transition input constant. The post-transition reference state $\hat{x}(t^+)$ is extended backward by flowing the dynamics backward in time while again holding the input constant. With these hybrid extensions, when there is a mode mismatch induced by a transition timing error, the reference is switched to the extension with the same hybrid mode.

In timestepping simulations, the effect of the hybrid transition is applied over several timesteps rather than instantaneously as in event-driven hybrid simulations. For example, when a contact is made, the penetrating velocities do not immediately go to zero and actually take several timesteps to go to zero. During these timesteps, the hybrid mode is not well defined. Because of this, the hybrid extension method does not work due to the timesteps that are “in between” hybrid modes. Instead, we propose to use a different approach for legged robots, where the constraint forces λ_j are used to scale the penalty on input from R_{min} to R_{max}

$$w_j = \frac{\lambda_j}{\sum_i \lambda_i} \quad (21)$$

$$R_j = R_{max} - w_j(R_{max} - R_{min}) \quad (22)$$

where j corresponds to the leg index. This modification penalizes changes in input less when a leg applies more ground reaction force and penalizes changes in input more when the leg applies less force to the ground. This is intuitive because when a leg is not supporting much weight, we want that leg to have lower gains because it has less control authority on the robot body.

B. Rollout and Forward Pass

Depending on the hybrid system, HiLQR MPC uses either an event-driven or timestepping simulation for its rollouts and forward passes. In this work, we demonstrate the cost mismatch update for an event-driven simulation on a bouncing ball. However, when multiple contacts are involved, as in the

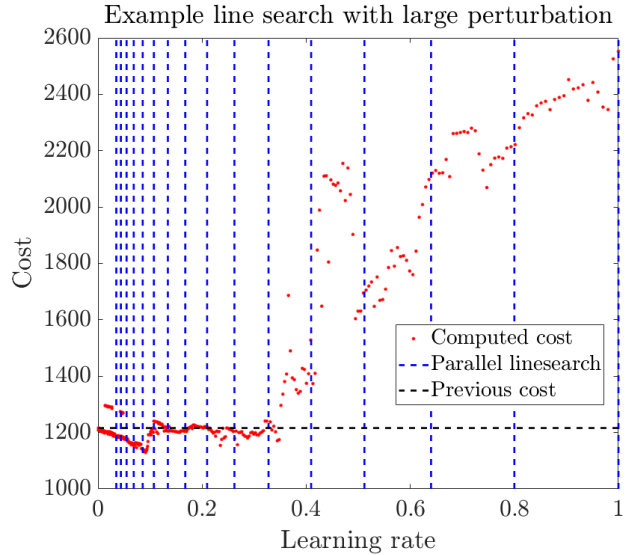


Figure 2: Linesearch for the first HiLQR MPC forward pass iteration after applying a $1.5\frac{m}{s}$ lateral perturbation while walking as shown in Fig 9. If computed sequentially, the linesearch would terminate after 12 steps.

case for a quadruped robot, simulating an event-driven system is significantly more difficult than using an out-of-the-box timestepping rigid body dynamics simulator. Many rigid body contact simulators utilize timestepping simulation methods. In this work, we use “Isaac Gym” (a high performance GPU-based physics simulation) [38], because the simulator has a unique feature where it can simulate multiple robots at once in an optimized fashion. We utilize parallel computations to parallelize the linesearch in the forward pass. An example linesearch is shown in Fig. 2, which shows the cost for different learning rates. Note that the cost is discontinuous with respect to the learning rate because the line search explores different contact sequences. In order for cost to be reduced in this case, the linesearch needs to take 12 steps if done sequentially. Due to the efficiency of parallel computations on the forward passes, parallelizing is on average twice as fast as computing the linesearch sequentially when comparing the computation times for the solutions in Fig. 9.

Several key implementation features consist of precomputing the gain schedule for the reference trajectory, reusing the valid portions of previous solutions, and always seeding the reference trajectory as one of the parallel solves in the linesearch.

Lastly, quaternion differences [39] are used instead of Euler angles when computing the orientation cost and linear feedback. This change allows for better convergence properties, as well as allowing for tracking more dynamic behaviors like the backflip in Fig. 1.

C. Backward Pass

The main challenge for the backward pass is how to compute the derivatives of the dynamics. For simple hybrid systems like the bouncing ball, the derivatives of the dynamics

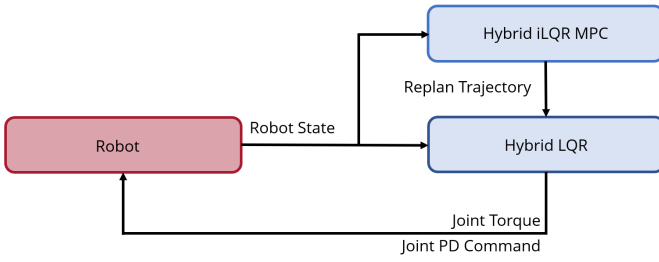


Figure 3: Hierarchy of controllers where HiLQR MPC is replanning trajectories as fast as possible while Hybrid LQR is tracking the most recent trajectory that was sent by HiLQR MPC.

and saltation matrix are trivial to find and compute [24]. However, computing the derivatives for the full order rigid body dynamics with unilateral constraints is not trivial – if done naively, the computations are incredibly slow. This is the same for the saltation matrix because it relies on computing the derivative of the impact map. In this work, we utilize a rigid body dynamics library called Pinocchio [40] (which computes these derivatives in an optimized fashion) for all full order contact rigid body dynamics derivatives.

For the backward pass, HiLQR MPC assumes the trajectory is produced by an event-driven simulation. If the timesteps are small enough, then approximating a timestepping simulation as an event-driven simulation on the backward pass is reasonable. Another approximation HiLQR MPC makes is that when simultaneous contacts are made during a timestep (i.e., 2 feet making contact at the same time), the contact sequencing is assumed to always follow the same contact order and to have happened at the end of the timestep. The chosen order is in increasing order of the indexing of the limbs. These approximations are validated through experimentation, where HiLQR MPC is still able to converge with these approximations in the presence of perturbations.

D. General Robot Implementation

For all robot experiments using HiLQR MPC, a 50 timestep MPC horizon is used with timesteps of 0.01 seconds. When running HiLQR MPC in simulation, the algorithm is able to pause the simulation in order to compute a new trajectory. Once a trajectory is generated, the first input of the planned trajectory is used as the control input for that timestep. Allowing HiLQR MPC to pause the simulation ensures that we can analyze how well the controller can perform independent of the computation time available. We also run the controller in real-time, because on hardware the dynamics cannot be paused.

To run HiLQR MPC in real-time for the physical robot implementation, several changes are made and hyper parameters are tuned to speed up the algorithm at the cost of performance. The first change is to run a hierarchy of controllers, as shown in Fig. 3, where a fast low level Hybrid LQR controller is run asynchronously from the trajectory generator (HiLQR MPC). HiLQR MPC runs separately as fast as possible and always

using the latest robot state. When solving for a new trajectory, sub-optimal trajectories are sent out at each forward pass iteration in order to send the low level controller the most recent trajectory modifications. If the current solve exceeds the maximum allotted time, the current solve is terminated and a new solve is started for the most recent robot state information. Several hyper-parameters are modified to reduce computation time, from reducing the number of robots running in parallel in the rollouts and forward passes to relaxing the optimality condition. Lastly, joint PD terms from the gain matrix are sent directly to the motor controller, which runs at 10KHz rather than computing the feedback at the Hybrid LQR level.

V. EXPERIMENTS

In this section, the experimental setups for HiLQR MPC are presented, with results given in Section VI. To validate the event-driven mode mismatch cost update, we first compare using the proposed update with not using any hybrid cost updates on a simple actuated bouncing ball hybrid system. Then, to show how this approach can scale up to a real system, simulated and physical robot experiments are carried out on a quadrupedal robot (Unitree A1) to compare HiLQR MPC with methods that use centroidal simplifications and Raibert heuristics for swing leg control: “Convex MPC” [10] and “Instant QP” [12–14]. Convex MPC returns ground reaction forces for the feet that are in contact with the ground and are subjected to friction constraints for a set horizon length. The dynamic model is a linearized floating base model and the optimization is formulated as a quadratic program. Instant QP solves the same problem, but for a single timestep. Because only one timestep is solved, Instant QP can update the solver with the actual contact condition of the feet and can provide more stability with respect to contact mismatches, but lacks the robustness that is gained from looking ahead.

A. Bouncing Ball

In this experiment, the same 1D bouncing ball hybrid system from [24] is used. The states of the system $x = [z, \dot{z}]^T$ are the vertical position z and the velocity \dot{z} and the input u is a force applied directly to the ball. The two hybrid modes, 1 and 2, are defined when the ball has a negative velocity $\dot{z} < 0$ and when the ball has a non-negative velocity $\dot{z} \geq 0$, respectively. The dynamics on each mode is ballistic dynamics plus the input

$$F_1(x, u) = F_2(x, u) := \left[\dot{z}, \frac{u}{m} - g \right]^T \quad (23)$$

Hybrid mode 1 transitions to 2 when the ball hits the ground, $g_{(1,2)}(x) := z$, and mode 2 transitions to 1 at the apex $g_{(2,1)}(x) := \dot{z}$. When mode 1 transitions to 2, an elastic impact is applied, $R_{(1,2)}(x) = [z, -e\dot{z}]^T$ where e is the coefficient of restitution. The reset map from 2 to 1 is identity. The event-driven simulation is implemented with MATLAB ODE 45 [41] with event detection.

To validate that updating the cost on mode mismatches improves convergence for HiLQR MPC, we first generate a reference trajectory using Hybrid iLQR to create an optimal

single bounce trajectory. HiLQR MPC is used to stabilize an initial large perturbation and is run with and without the hybrid cost update for event-driven simulations. For both cases, HiLQR MPC is applied at every timestep. At each timestep, convergence is recorded where convergence is determined by the expected reduction (19). For this test, the convergence cut-off is set to be $\delta J < 1e^{-4}$. It is expected that, by utilizing the mode extensions, convergence will improve because the algorithm will not spend unnecessary computation and effort in flipping the velocity of the ball if there is a mismatch in impact timing, rather it will wait for when the impact applies the flip.

B. Simulated Robot Controller Comparison

To demonstrate the robustness of cohesively planning whole body motions and allowing contact schedules to change, we compare HiLQR MPC to Convex MPC and Instant QP by applying perturbations to A1 while implementing a walking gait in simulation. To make the comparison fair, the walking gait that HiLQR MPC is tracking is the same one generated from Convex MPC in the absence of perturbations. Similar gait parameters are chosen for Instant QP to produce a similar gait. All controllers are run at each timestep and use the first control input of the new trajectory as the control input for that timestep.

The walking gait starts from a standing pose and then attempts to reach a desired forward velocity of $0.2 \frac{m}{s}$. Lateral velocity perturbations are applied to the robot's body at two different magnitudes and eight different times along the gait cycle: four when each foot is in swing when getting up to speed and the other four when the gait is in steady state. The number of times the robot falls and the maximum perturbed lateral position are recorded for each push.

It is expected that HiLQR MPC should be able to recover from a wider variety of perturbations and have less deviation when the perturbations are large when compared against the centroidal methods because it can utilize the nonlinear contact dynamics of the swing and stance legs cohesively.

C. Physical Robot Controller Comparison

The bulk of the analysis for comparing the controllers is done in simulation because the perturbations can be consistently applied in both cases with a variety of different perturbations. To reliably apply the same perturbation on hardware, we opt for a consistent motor command block for a short period of time while the robot is walking. Once the motor commands are unblocked, the controller must react to the robot falling over, catch itself, and then continue walking.

In this experiment, we compare HiLQR MPC against Instant QP, where both controllers are able to handle the perturbation in simulation but come up with different solutions. HiLQR MPC tends to replan a stand trajectory after it realizes that it is falling to catch itself, while Instant QP tries to continue the walking gait and recirculates the legs in order to catch itself. The perturbation is applied shortly after walking has started, and the torque commands are blocked for 0.15 seconds. The experiment is run 5 times for each controller and failure is

determined by if the robot's body hits the floor and if the controller is able to continue walking after the perturbation. For state estimation, we use the Kalman filter from [42]. Because HiLQR MPC creates a new plan to track in order to handle the perturbation, it is expected to outperform Instant QP which is trying its best to continue walking.

VI. RESULTS

In this section, we review the results for each experiment. Overall, utilizing the cost mismatch updates is crucial for obtaining good solutions, and HiLQR MPC can withstand large perturbations by modifying the contact sequence in an optimal manner.

A. Bouncing ball HiLQR MPC

The task for the bouncing ball experiment, detailed in Sec. V-A, is to track a predefined trajectory using HiLQR MPC for a fully actuated bouncing ball. The target trajectory is 1 second long, where the ball starts at 4 meters above the ground with no velocity and ends at 2.5 meters above the ground with no velocity. We compare using the event-driven hybrid cost update (Sec. IV-A) to not using this update, and the results of this experiment are shown in Fig. 4.

As expected, both methods converge and track well before the impact event is within the horizon of the HiLQR MPC. The approaches differ once the hybrid event is within the horizon, as can be seen by the high control effort and unnatural kink in state space that is produced when not using the cost update. Furthermore, of the 1001 time steps, 8 did not converge when the cost update was not used. Although the number of unconverged timesteps is small, the quality of the trajectory suffered greatly, as shown in Fig. 4, top row. This is because without updating the cost to account for hybrid mode mismatches, the gradient information biases the solution towards flipping the velocity before impact.

Using the cost update for hybrid mode mismatches, HiLQR MPC can correctly utilize the impact to reduce tracking error, as shown in Fig. 4, bottom row. The cost update allows HiLQR MPC to create plans that are closer to the target trajectory by shifting contact times rather than making large modifications to the input to match the contact schedule, which results in significantly better convergence. In addition to having better tracking performance, when using trajectory optimization for MPC, it is desirable to always converge and to not make drastic changes from the planned trajectory unless necessary.

B. Simulated Robot Controller Comparison

The robustness of HiLQR MPC is compared with Convex MPC and Instant QP for a walking trajectory at eight different perturbations in simulation as discussed in Sec. V-B. The results are summarized in Table I, farthest perturbed position is visualized for each experiment in Figs. 5 and 6, change in contact sequence in Figs. 7 and 8, and the resulting behavior shown in Fig 9.

As expected, deviations from the smaller perturbation lead to similar results and high success for all controllers. This

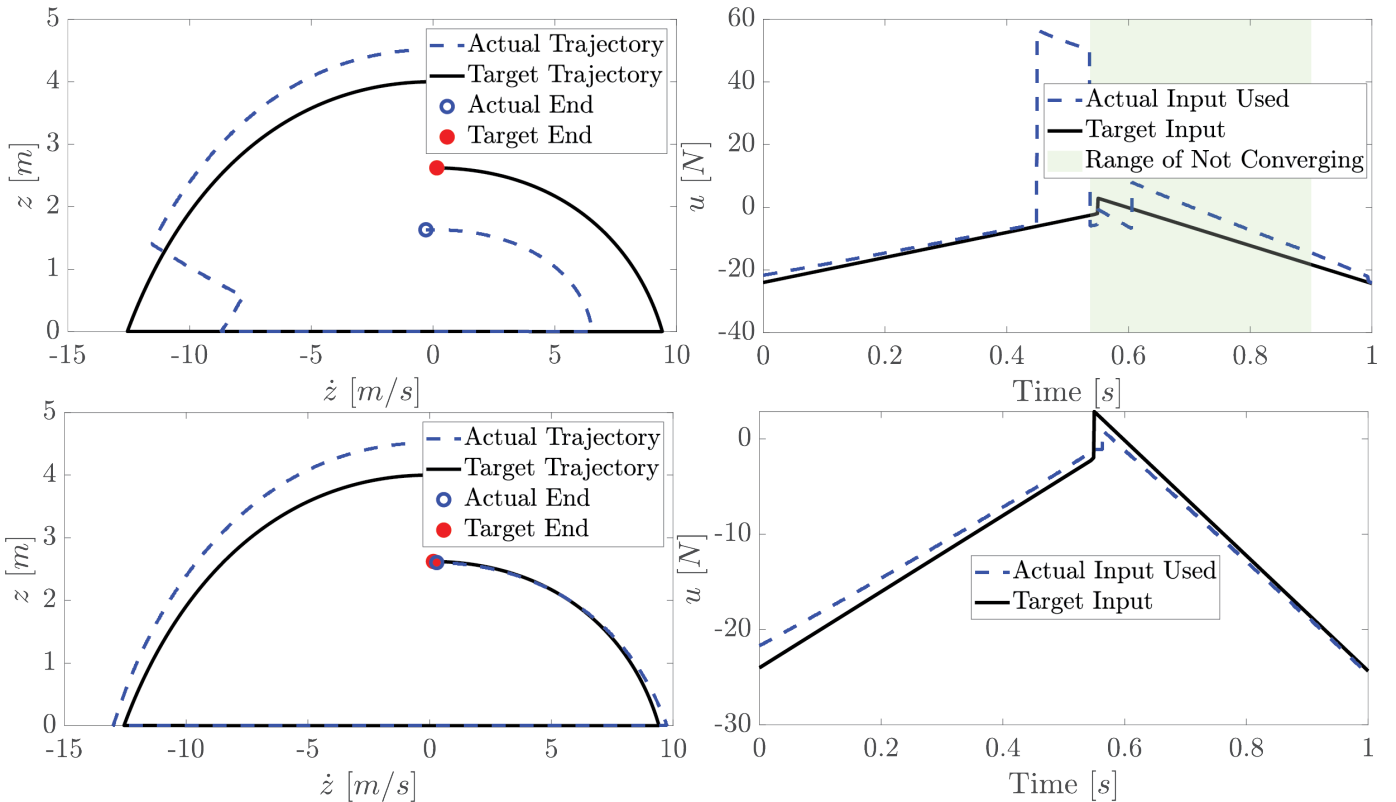


Figure 4: Comparing HiLQR MPC not using the event-driven hybrid cost update (top row) and using the event-driven hybrid cost update (bottom row) where the state space trajectory tracking is shown in (left column) and input usage in time series is shown in (right column). HiLQR solutions are shown in (blue dashed) and the target trajectory is shown in (black solid). The end of trajectories are denoted with (circle). When not using the event-driven hybrid cost update the trajectory tracking suffered, as evident by the high input effort and sharp deviations in trajectory that attempt to track the post-impact velocity before the impact occurs. Several solutions did not converge as shown in with (green highlight). Whereas, using the event-driven hybrid cost update led to altogether better convergence and tracking.

is most likely because the perturbations do not require the controller to heavily modify the trajectory while stabilizing less stable robot states, such as in the case of the larger perturbations. In the medium and large perturbation experiments, HiLQR MPC had a higher success rate of 100% and 88% compared to the centroidal methods – Convex MPC 88% and 50% and Instant QP 50% and 25%. Failure for the controllers tended to occur when a right leg was in swing (both front right and back). This failure mode is most likely due to the lateral perturbation being applied in the left direction causing the stabilizing maneuvers to be more complicated and less stable. Because HiLQR MPC is able to plan the body and swing legs more cohesively, it can handle these complex maneuvers better than the centroidal methods, where the stance and swing legs are planned separately. This difference is mostly highlighted when the perturbations are larger. Since Instant QP performed worse than Convex MPC, further comparisons are made only between HiLQR MPC and Convex MPC.

In the large perturbation experiments, HiLQR MPC deviated half as much as Convex MPC when comparing max lateral deviations in body position, as shown in Table I. An example trial (large perturbation during the first step) is shown in Fig. 9, where HiLQR MPC used less steps to stabilize the pertur-

Table I: Lateral perturbation success rates for a medium perturbation $1.0m/s$, a large perturbation $1.5m/s$, and the average max deviation for the large perturbation over 8 trials.

Controller	1.0m/s Succ. [%]	1.5m/s Succ. [%]	Avg. Dev. [m]
HiLQR MPC	100%	88%	0.512m
Convex MPC	88%	50%	1.032m
Instant QP	50%	25%	3.729m

bation, which ultimately led to the body deviating less than half of the deviation from Convex MPC. The contact sequence for the reference and the initial solution after applying the perturbation are shown in Figures 7 and 8. Note that HiLQR MPC is solving for new trajectories that modify the contact sequence in order to better stabilize the behavior rather than adhering to the original plan's contact sequence. This is crucial because HiLQR MPC can add or remove contacts to help catch itself, as well as optimize the new contact locations.

Overall, HiLQR MPC performed similarly to or better than Convex MPC when stabilizing perturbations along a walking trajectory. When the perturbations are large, HiLQR MPC outperforms Convex MPC because it is able to replan a new contact sequence to stabilize about and it can fully utilize the

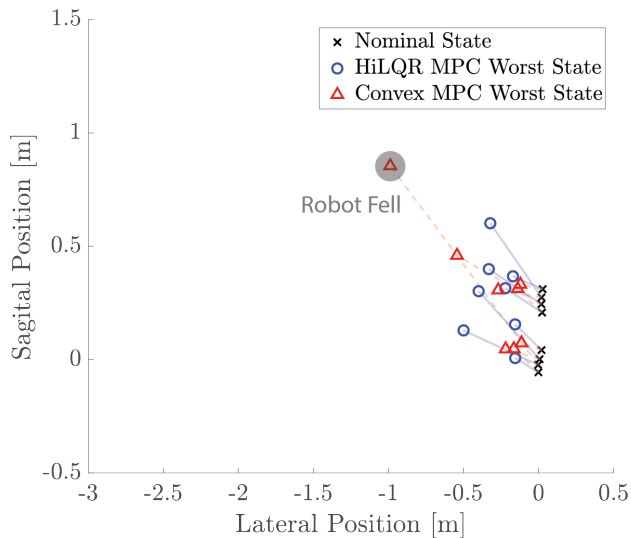


Figure 5: Medium perturbation (1.0 m/s lateral perturbation). Plots the nominal trajectory and worst case error in lateral position for both controllers.

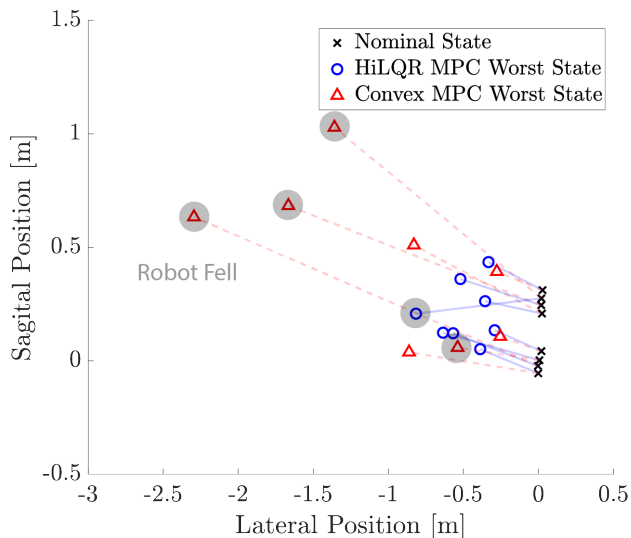


Figure 6: Large perturbation (1.5 m/s lateral perturbation). Plots the nominal trajectory and worst case error in lateral position for both controllers.

nonlinear dynamics for the more aggressive maneuvers.

C. Physical Robot Controller Comparison

The results of the motor-blocking physical robot experiment from Sec. V-C – where the motor commands were blocked for 150 milliseconds shortly after the walk started and HiLQR is compared to Instant QP over five trials – are shown in Fig. 10 and Table II. Over five trials, HiLQR MPC was able to stabilize successfully after the motor block was released every time, while Instant QP was completely unstable 60% of the time and 40% of the time was able to stand up and walk after the body hit the ground. Two unintended additional perturbations occurred in this experiment – there is a consistent 10 millisecond input delay on A1 and another perturbation

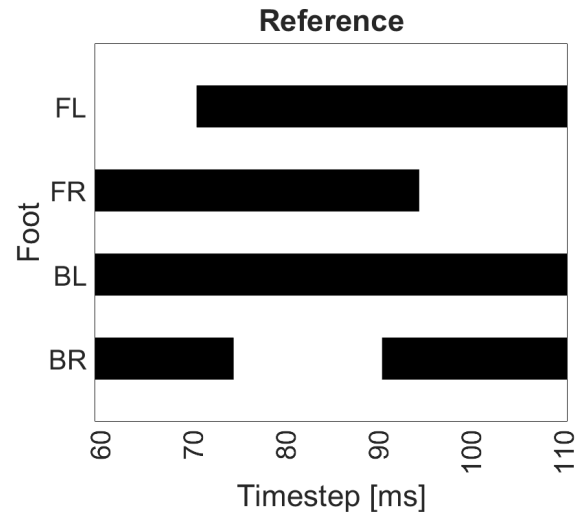


Figure 7: Hildebrand diagram for the nominal walking gait where black means the foot is in contact.

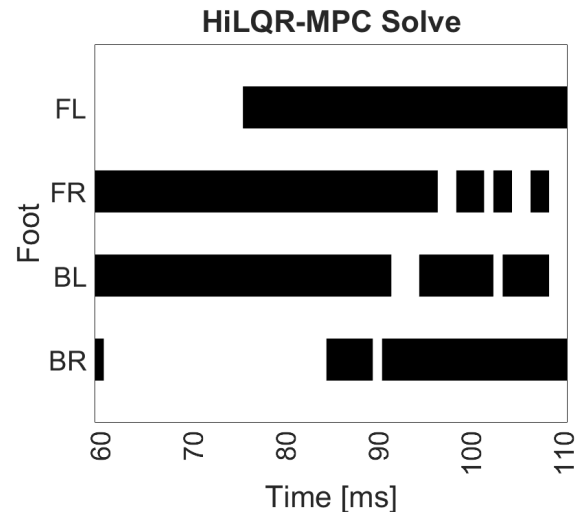


Figure 8: Hildebrand diagram for a single solve of HiLQR MPC rejecting the large perturbation at 60 ms as shown in the top of Fig. 9 where black means the foot is in contact. See that HiLQR MPC is removing and adding back contacts when advantageous to help stabilize the behavior.

caused by the state estimator. The estimator relies on the kinematic information from the legs that are in contact to get a better estimate of the robot body. However, when the motor commands were blocked, all the contact forces went close to zero, which resulted in a degraded estimate of the robot body until the legs made sufficient contact with the ground again.

HiLQR MPC was able to replan a stand trajectory in order to catch itself rather than sticking to the original plan of walking as Instant QP. In the times that Instant QP successfully rejected the perturbation, the robot body actually hits the ground and the legs that are planned to be in stance apply enough standing force to get back up while the back right leg recirculates in order to counteract the backward velocity induced by getting back up. Since this relies on the body hitting the ground

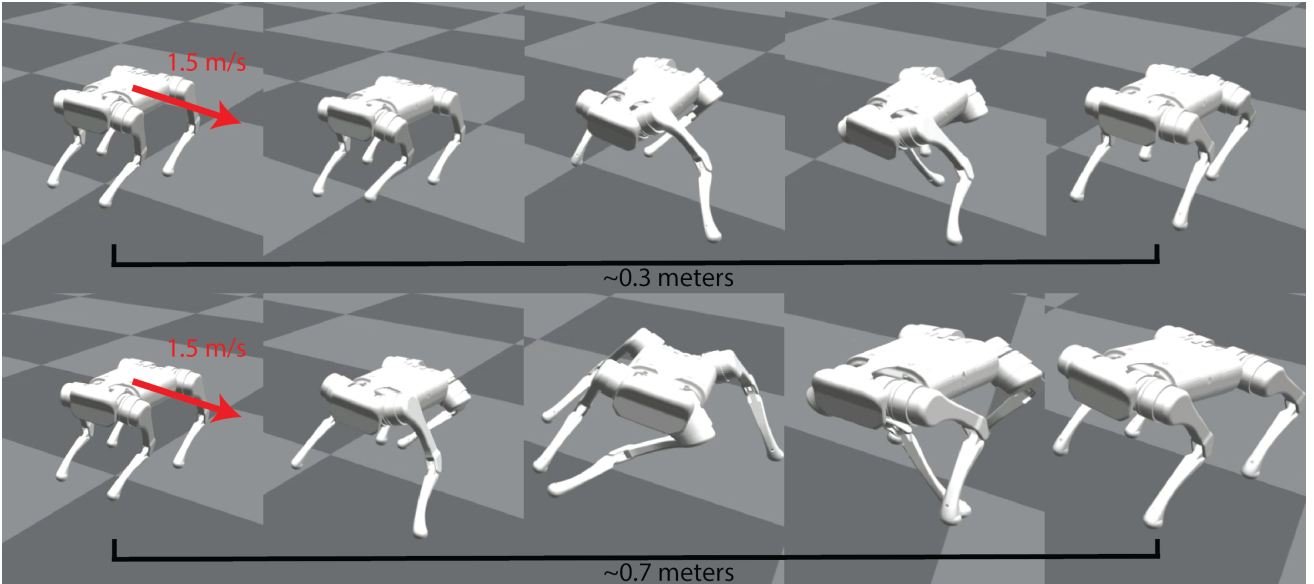


Figure 9: Applying 1.5 m/s lateral perturbation during the first step of the walking gait. (Top row) shows HiLQR MPC recovering from the perturbation in one step and accruing a lateral deviation of 0.3 meters while (bottom row) shows Convex MPC taking several steps to handle the perturbation and is perturbed 0.7 meters away from the nominal.

Table II: Motor blocking perturbation results over 5 trials.

Controller	Success	Hit Ground	Uncontrolled
HiLQR MPC	100%	0%	0%
Instant QP	0%	40%	60%

correctly and the back leg perfectly stabilizing the motion, it is a lot less reliable but is able to catch itself occasionally.

Similarly to the simulated experiments, HiLQR MPC outperforms the centroidal method (Instant QP) because HiLQR MPC does not have to adhere to a rigid gait schedule and can fluidly replan a new contact sequence to help stabilize the perturbation. Although Instant QP utilizes the current contact information to inform which legs are in contact, the controller is trying its best to follow the scheduled gait sequence. In this case, modifying the gait sequence from a walk to a stand is much more reliable. HiLQR MPC is able to track the walking gait when appropriate but modify it to a stand if needed to catch the robot and seamlessly return to walking once the perturbation has been stabilized. Having the ability to automatically modify the gait schedule to generate these stabilizing behaviors is important for a controller because the initial plan might not always be the best in the presence of disturbances.

VII. DISCUSSION

Allowing for varying contact sequences while planning for the full nonlinear dynamics of a robotic system is very difficult, but leads to more robust control. In this work, we extend Hybrid iLQR to work as a model predictive controller, which can vary the contact sequence of the target trajectory as well as plan with the nonlinear dynamics. This extension is made possible by fixing gradient issues that occur when there

are hybrid mode mismatches, using fast analytical derivatives of the contact dynamics, and parallelizing the line search in the forward pass.

In simulation, HiLQR MPC outperforms the state of the art centroidal motion planning technique (Convex MPC) for stabilizing perturbations 88% success rate vs 50% for large perturbations and 100% vs 88% for medium perturbations. This is because HiLQR MPC is able to fully utilize the legs of the robot to help catch itself and can create more efficient and elegant solutions, needing fewer steps to recover.

HiLQR MPC is also able to run in real-time with some modifications to the hyperparameters and utilizing a hierarchical control structure where trajectories are sent to a lower level Hybrid LQR controller to track the hybrid trajectories planned by HiLQR MPC. We are able to show for a motor blocking perturbation that HiLQR MPC is able to withstand this better than Instant QP, where HiLQR MPC succeeded for all trials and Instant QP could only stabilize 40% of the time (and even then only after the robot body hit the ground). The high success rate for HiLQR MPC is due to planning a reliable catching behavior, while Instant QP is continuously attempting to walk as best it can.

The code is currently implemented in Python while using several C++ libraries that utilize Python wrappers. Improvements in the real-time application will be seen by further optimizing the code and implementing it in C++. Overall, HiLQR MPC is a very modular model predictive controller which can be run for any hybrid dynamical system of type Def. 1. Besides the hybrid dynamical systems definition, there are no restrictive simplifications that are made, which makes the controller generalizable to many different behaviors. Future work will add additional constraints through Augmented Lagrangian [43] for obstacle avoidance and actuator constraints.

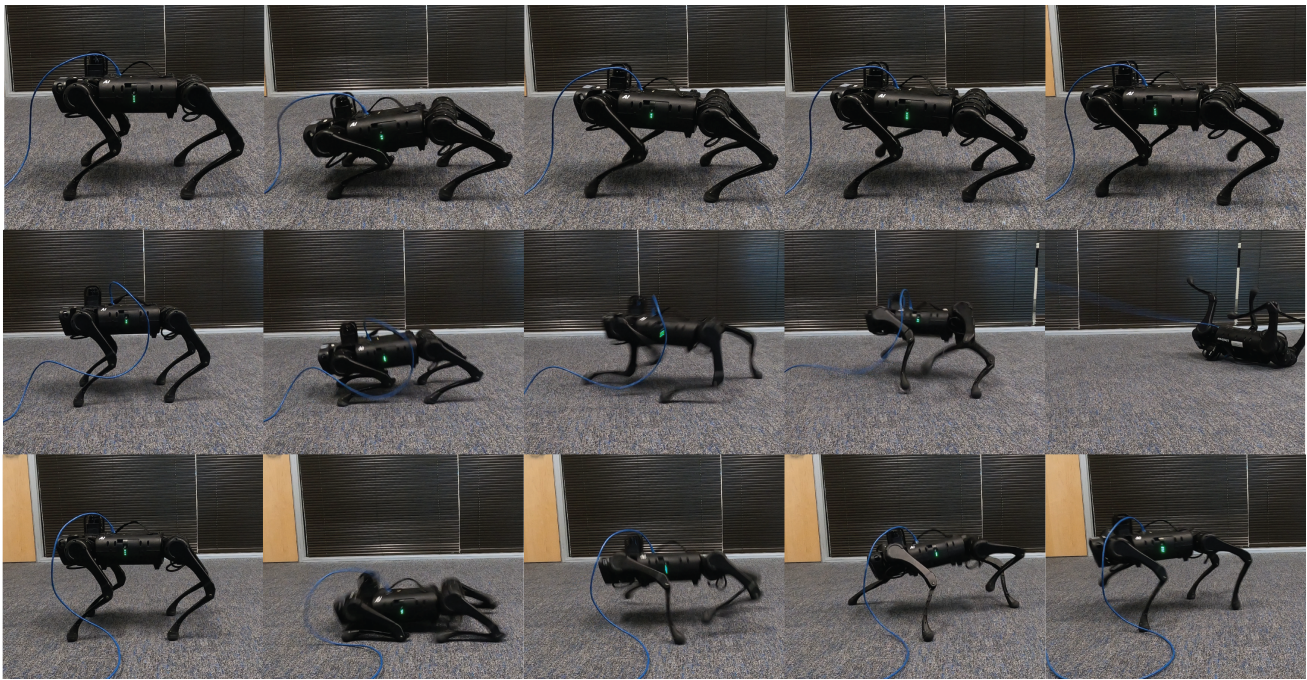


Figure 10: Turning off motor commands for 150 ms during the first step. HiLQR MPC (top row) creates a catching behavior and then goes back into the scheduled walk. Instant QP sometimes tries to step to regulate velocity which destabilizes the robot (middle row). Other times, Instant QP hits the ground (bottom row), which stabilizes the body velocities and the robot is able to shoot its legs out in order to get back into the walk.

REFERENCES

- [1] M. Posa, C. Cantu, and R. Tedrake, “A direct method for trajectory optimization of rigid bodies through contact,” *The International Journal of Robotics Research*, vol. 33, no. 1, pp. 69–81, 2014.
- [2] I. Mordatch, E. Todorov, and Z. Popović, “Discovery of complex behaviors through contact-invariant optimization,” *ACM Transactions on Graphics*, vol. 31, no. 4, p. 43, 2012.
- [3] K. Mombaur, “Using optimization to create self-stable human-like running,” *Robotica*, vol. 27, no. 3, pp. 321–330, 2009.
- [4] M. Diehl, H. G. Bock, H. Diedam, and P.-B. Wieber, “Fast direct multiple shooting algorithms for optimal robot control,” in *Fast motions in biomechanics and robotics*. Springer, 2006, pp. 65–93.
- [5] O. Von Stryk, “User’s guide for DIRCOL—a direct collocation method for the numerical solution of optimal control problems,” Technische Universitat Darmstadt, Tech. Rep., 1999.
- [6] M. Posa, S. Kuindersma, and R. Tedrake, “Optimization and stabilization of trajectories for constrained dynamical systems,” in *IEEE International Conference on Robotics and Automation*, May 2016, pp. 1366–1373.
- [7] M. Kelly, “An introduction to trajectory optimization: How to do your own direct collocation,” *SIAM Review*, vol. 59, no. 4, pp. 849–904, 2017.
- [8] D. Pardo, M. Neunert, A. W. Winkler *et al.*, “Hybrid direct collocation and control in the constraint-consistent subspace for dynamic legged robot locomotion.” in *Robotics: Science and Systems*, vol. 10, 2017.
- [9] A. W. Winkler, C. D. Bellicoso, M. Hutter, and J. Buchli, “Gait and trajectory optimization for legged systems through phase-based end-effector parameterization,” *IEEE Robotics and Automation Letters*, vol. 3, no. 3, pp. 1560–1567, 2018.
- [10] J. Di Carlo, P. M. Wensing, B. Katz *et al.*, “Dynamic locomotion in the MIT Cheetah 3 through convex model-predictive control,” in *IEEE/RSJ International Conference on Intelligent Robots and Systems*, 2018, pp. 1–9.
- [11] D. Kim, J. Di Carlo, B. Katz *et al.*, “Highly dynamic quadruped locomotion via whole-body impulse control and model predictive control,” *arXiv preprint arXiv:1909.06586*, 2019.
- [12] X. Da, Z. Xie, D. Hoeller *et al.*, “Learning a contact-adaptive controller for robust, efficient legged locomotion,” in *Conference on Robot Learning*, 16–18 Nov 2020, pp. 883–894.
- [13] Z. Xie, X. Da, B. Babich *et al.*, “Glide: Generalizable quadrupedal locomotion in diverse environments with a centroidal model,” *arXiv preprint arXiv:2104.09771*, 2021.
- [14] C. Gehring, S. Coros, M. Hutter *et al.*, “Control of dynamic gaits for a quadrupedal robot,” in *IEEE international conference on Robotics and automation*, 2013, pp. 3287–3292.
- [15] M. H. Raibert, *Legged robots that balance*. MIT press, 1986.
- [16] J. Pratt, J. Carff, S. Drakunov, and A. Goswami, “Capture

- point: A step toward humanoid push recovery,” in *IEEE-RAS International Conference on Humanoid Robots*, 2006, pp. 200–207.
- [17] D. Mayne, “A second-order gradient method for determining optimal trajectories of non-linear discrete-time systems,” *International Journal of Control*, vol. 3, no. 1, pp. 85–95, 1966.
- [18] W. Li and E. Todorov, “Iterative linear quadratic regulator design for nonlinear biological movement systems,” in *International Conference on Informatics in Control, Automation and Robotics*, 2004, pp. 222–229.
- [19] Y. Tassa, T. Erez, and E. Todorov, “Synthesis and stabilization of complex behaviors through online trajectory optimization,” in *IEEE/RSJ International Conference on Intelligent Robots and Systems*, 2012.
- [20] H. Li and P. M. Wensing, “Hybrid systems differential dynamic programming for whole-body motion planning of legged robots,” *IEEE Robotics and Automation Letters*, vol. 5, no. 4, pp. 5448–5455, 2020.
- [21] C. Mastalli, R. Budhiraja, W. Merkt *et al.*, “Crocodyl: An efficient and versatile framework for multi-contact optimal control,” in *IEEE International Conference on Robotics and Automation*, 2020, pp. 2536–2542.
- [22] H. Li, R. J. Frei, and P. M. Wensing, “Model hierarchy predictive control of robotic systems,” *IEEE Robotics and Automation Letters*, vol. 6, no. 2, pp. 3373–3380, 2021.
- [23] S. Le Cleac’h, T. A. Howell, M. Schwager, and Z. Manchester, “Fast contact-implicit model-predictive control,” *arXiv preprint arXiv:2107.0561*, 2021.
- [24] N. J. Kong, G. Council, and A. M. Johnson, “iLQR for piecewise-smooth hybrid dynamical systems,” in *IEEE Conference on Decision and Control*, December 2021.
- [25] A. M. Johnson, S. A. Burden, and D. E. Koditschek, “A hybrid systems model for simple manipulation and self-manipulation systems,” *The International Journal of Robotics Research*, vol. 35, no. 11, 2016.
- [26] A. Back, J. M. Guckenheimer, and M. Myers, “A dynamical simulation facility for hybrid systems,” in *Hybrid Systems*, ser. Lecture Notes in Computer Science. Springer Berlin / Heidelberg, 1993, vol. 736.
- [27] J. Lygeros, K. H. Johansson, S. N. Simic *et al.*, “Dynamical properties of hybrid automata,” *IEEE Transactions on Automatic Control*, vol. 48, no. 1, pp. 2–17, 2003.
- [28] R. Goebel, R. G. Sanfelice, and A. R. Teel, “Hybrid dynamical systems,” *IEEE control systems magazine*, vol. 29, no. 2, pp. 28–93, 2009.
- [29] M. A. Aizerman and F. R. Gantmacher, “Determination of stability by linear approximation of a periodic solution of a system of differential equations with discontinuous right-hand sides,” *The Quarterly Journal of Mechanics and Applied Mathematics*, vol. 11, no. 4, 1958.
- [30] R. Leine and H. Nijmeijer, *Dynamics and bifurcations of non-smooth mechanical systems*. Springer, 2004.
- [31] M. Rijnen, A. Saccon, and H. Nijmeijer, “On optimal trajectory tracking for mechanical systems with unilateral constraints,” in *IEEE Conference on Decision and Control*, 2015, pp. 2561–2566.
- [32] S. A. Burden, T. Libby, and S. D. Coogan, “On contraction analysis for hybrid systems,” 2018, arXiv:1811.03956.
- [33] R. A. Wehage and E. J. Haug, “Dynamic analysis of mechanical systems with intermittent motion,” *Journal of Mechanical Design*, vol. 104, no. 4, pp. 778–784, 10 1982.
- [34] F. Pfeiffer and C. Glocker, *Multibody dynamics with unilateral contacts*. John Wiley & Sons, 1996.
- [35] B. Brogliato, A. Ten Dam, L. Paoli *et al.*, “Numerical simulation of finite dimensional multibody nonsmooth mechanical systems,” *Appl. Mech. Rev.*, vol. 55, no. 2, pp. 107–150, 2002.
- [36] D. E. Stewart and J. C. Trinkle, “An implicit time-stepping scheme for rigid body dynamics with inelastic collisions and coulomb friction,” *International Journal for Numerical Methods in Engineering*, vol. 39, no. 15, pp. 2673–2691, 1996.
- [37] M. Anitescu and F. A. Potra, “Formulating dynamic multi-rigid-body contact problems with friction as solvable linear complementarity problems,” *Nonlinear Dynamics*, vol. 14, no. 3, pp. 231–247, 1997.
- [38] V. Makovychuk, L. Wawrzyniak, Y. Guo *et al.*, “Isaac Gym: High performance GPU based physics simulation for robot learning,” in *Conference on Neural Information Processing Systems, Datasets and Benchmarks Track*, 2021.
- [39] B. E. Jackson, K. Tracy, and Z. Manchester, “Planning with attitude,” *IEEE Robotics and Automation Letters*, vol. 6, no. 3, pp. 5658–5664, 2021.
- [40] J. Carpentier, F. Valenza, N. Mansard *et al.*, “Pinocchio: fast forward and inverse dynamics for poly-articulated systems,” <https://stack-of-tasks.github.io/pinocchio>, 2015–2021.
- [41] L. F. Shampine, I. Gladwell, L. Shampine, and S. Thompson, *Solving ODEs with MATLAB*. Cambridge University Press, 2003.
- [42] G. Bledt, P. M. Wensing, S. Ingersoll, and S. Kim, “Contact model fusion for event-based locomotion in unstructured terrains,” in *IEEE International Conference on Robotics and Automation*, 2018, pp. 4399–4406.
- [43] T. A. Howell, B. E. Jackson, and Z. Manchester, “Altro: A fast solver for constrained trajectory optimization,” in *IEEE/RSJ International Conference on Intelligent Robots and Systems*, 2019, pp. 7674–7679.